BIOLOGY OF REPRODUCTION (2013) **89**(2):44, 1–13
Published online before print 17 July 2013.
DOI 10.1095/biolreprod.113.110221

Prophase I Mouse Oocytes Are Deficient in the Ability to Respond to Fertilization by Decreasing Membrane Receptivity to Sperm and Establishing a Membrane Block to Polyspermy[1]

Cassie A. Kryzak,[3] Maia M. Moraine,[3] Diane D. Kyle,[3] Hyo J. Lee,[3] Caelin Cubeñas-Potts,[3] Douglas N. Robinson,[4] and Janice P. Evans[2,3]

[3]*Department of Biochemistry and Molecular Biology, Bloomberg School of Public Health, Johns Hopkins University, Baltimore, Maryland*
[4]*Department of Cell Biology, School of Medicine, Johns Hopkins University, Baltimore, Maryland*

ABSTRACT

Changes occurring as the prophase I oocyte matures to metaphase II are critical for the acquisition of competence for normal egg activation and early embryogenesis. A prophase I oocyte cannot respond to a fertilizing sperm as a metaphase II egg does, including the ability to prevent polyspermic fertilization. Studies here demonstrate that the competence for the membrane block to polyspermy is deficient in prophase I mouse oocytes. In vitro fertilization experiments using identical insemination conditions result in monospermy in 87% of zona pellucida (ZP)-free metaphase II eggs, while 92% of ZP-free prophase I oocytes have four or more fused sperm. The membrane block is associated with a postfertilization reduction in the capacity to support sperm binding, but this reduction in sperm-binding capacity is both less robust and slower to develop in fertilized prophase I oocytes. Fertilization of oocytes is dependent on the tetraspanin CD9, but little to no release of CD9 from the oocyte membrane is detected, suggesting that release of CD9-containing vesicles is not essential for fertilization. The deficiency in membrane block establishment in prophase I oocytes correlates with abnormalities in two postfertilization cytoskeletal changes: sperm-induced cortical remodeling that results in fertilization cone formation and a postfertilization increase in effective cortical tension. These data indicate that cortical maturation is a component of cytoplasmic maturation during the oocyte-to-egg transition and that the egg cortex has to be appropriately primed and tuned to be responsive to a fertilizing sperm.

activation competence, block to polyspermy, CD9, cytoplasmic maturation, polyspermy

INTRODUCTION

The oocyte-to-egg transition is a critical part of successful reproduction and development. Mammalian oocytes undergo a transition known as meiotic maturation (also called oocyte maturation) coincident with ovulation [1]. One key part of this maturation process is known as nuclear maturation, in which the oocyte undergoes the first meiotic division and then progresses to metaphase of meiosis II. Another component of oocyte maturation, sometimes referred to as cytoplasmic maturation, is the acquisition of activation competence (i.e., competence to undergo egg activation upon fertilization) and developmental competence. These cellular and molecular changes during meiotic maturation result in a metaphase II egg that is fully capable of being fertilized and of responding to a fertilizing sperm and progressing through the egg-to-embryo transition and embryonic development [2–5].

Several responses to the fertilizing sperm, and the cellular mechanisms underlying these responses, are lacking, deficient, or aberrant in prophase I oocytes. One of these is the ability to release Ca^{2+} from intracellular stores to the cytoplasm. Fertilized metaphase II eggs undergo repetitive sperm-induced transient increases in cytosolic Ca^{2+} concentrations ($[Ca^{2+}]_{cyt}$), whereas sperm-induced increases in $[Ca^{2+}]_{cyt}$ in fertilized prophase I oocytes are dramatically reduced [6–8]. Several components of the Ca^{2+}-signaling system, both upstream and downstream of Ca^{2+} release, change during meiotic maturation for maximum responsiveness in the metaphase II egg. These include increased Ca^{2+} stores, reorganization of the endoplasmic reticulum, increased CaMKII activity, and changes in the amount, sensitivity, and localization of the inositol 1,4,5-triphosphate receptor [7–15]. Beyond Ca^{2+}-signaling capacity, there are other changes that are critical for successful embryogenesis to occur during the oocyte-to-egg transition. The ability to decondense sperm chromatin develops during this time [16, 17]. The molecular mechanisms of cell volume regulation, an essential process for cell viability, change dramatically from oocyte to egg to embryo. Early embryos require the activity of the glycine-specific transporter SLC6A9 (also known as GLYT1), which is quiescent in prophase I oocytes and becomes active with meiotic maturation occurring with ovulation [18–20]. Euploidy is also crucial for successful embryo development. Prevention of polyspermic fertilization is a key process for achieving embryonic euploidy, and the blocks to polyspermy are part of the normal egg activation responses in fertilized metaphase II eggs. As addressed in the research presented here, the ability to prevent polyspermic fertilization develops during the oocyte-to-egg transition, building on evidence that insemination of immature oocytes results in high levels of polyspermy in multiple mammalian species [3, 6, 21, 22].

One mechanism of preventing polyspermic fertilization is the zona pellucida (ZP) block to polyspermy, which occurs as a result of increased cytosolic Ca^{2+} in the fertilized egg. Increased $[Ca^{2+}]_{cyt}$ induces exocytosis of cortical granules, in turn causing a conversion of the ZP from a form that supports

[1]Supported by R01 HD045671 from the National Institutes of Health to J.P.E.
[2]Correspondence: Janice P. Evans, Department of Biochemistry and Molecular Biology, Bloomberg School of Public Health, 615 N. Wolfe St., Johns Hopkins University, Baltimore, MD 21205.
E-mail: jpevans@jhsph.edu

Received: 21 April 2013.
First decision: 8 May 2013.
Accepted: 8 July 2013.

eISSN: 1529-7268 http://www.biolreprod.org
ISSN: 0006-3363

sperm binding to a form that is less supportive of sperm binding [23–25]. However, in fertilized prophase I oocytes, very little cortical granule exocytosis occurs [3, 26–29], attributable perhaps in part to the blunted $[Ca^{2+}]_{cyt}$ increase in fertilized prophase I oocytes [6–8]. However, prophase I mouse oocytes injected with an extract of soluble sperm proteins, which induces transient $[Ca^{2+}]_{cyt}$ increases mimicking those in normal fertilized metaphase II eggs, still do not undergo cortical granule exocytosis [14, 30, 31]. The competence to undergo cortical granule exocytosis is acquired during meiotic maturation and is associated with multiple events, including translocation of cortical granules to the plasma membrane, cortical granule docking to the plasma membrane, and organization of SNARE complexes with cortical granules [14, 32].

This study focuses on the membrane block to polyspermy. Mehlmann and Kline [6], in studies of fertilization-induced Ca^{2+} release in prophase I oocytes, observed that ZP-free prophase I oocytes tended to be more polyspermic than ZP-free metaphase II eggs. This, combined with our own observations, prompted us to hypothesize that the ability to establish a membrane block to polyspermy develops as part of acquisition of activation competence during meiotic maturation. The membrane block to polyspermy, similar to the ZP block, involves the postfertilization conversion of the egg plasma membrane to a state that is less receptive to sperm. Fertilized, monospermic eggs recovered from natural matings have extra sperm in the perivitelline space (PVS, i.e., between the ZP and the plasma membrane), apparently unable to fertilize the egg despite being in close proximity to the membrane (e.g., [33, 34]; other references in [35, 36]). Some species' eggs (e.g., rabbit) have high numbers of sperm in the PVS [37, 38], indicative of a highly effective membrane block and relatively less contribution of a ZP block. Other species (mouse, human, rat, guinea pig, cat, ferret, pig, cattle) appear to utilize both blocks to polyspermy, based on the presence of ~1–10 supernumerary sperm found in the PVS of early embryos, suggestive of an effective membrane block, and also a ZP block to limit the number of sperm reaching the PVS [33–35, 39–41]. Additionally, in vitro fertilization (IVF) experiments demonstrate that ZP-free mammalian zygotes show reduced penetration by additional sperm [40, 42–45].

The mammalian membrane block differs from the membrane block in nonmammalian animal species (also known as the fast block in these species) because the membrane block in mammalian eggs does not appear to require a rapid and transient depolarization of the egg membrane potential [46–50]. In mouse embryos, the sperm-induced increase in $[Ca^{2+}]_{cyt}$ facilitates the conversion of the membrane to a state that is unreceptive to sperm [51, 52], but increased $[Ca^{2+}]_{cyt}$ is not sufficient for membrane block establishment. Parthenogenetic increases in $[Ca^{2+}]_{cyt}$, including those that faithfully mimic the characteristics of sperm-induced Ca^{2+} transients, do not trigger membrane block establishment [44, 51, 53, 54]. Fertilization by intracytoplasmic sperm injection (ICSI) also does not induce membrane block establishment, not even in our studies in which we used improved ICSI techniques for optimal Ca^{2+} signals and developmental potential [54–56].

The overall goal of this study is to test the hypothesis that the ability to establish a membrane block to polyspermy develops as part of acquisition of activation competence during meiotic maturation. We first present studies that significantly extend observations of increased polyspermy in ZP-free prophase I mouse oocytes [6]. These data reveal defects in the timing and the robustness of the conversion of the prophase I oocyte plasma membrane to an unreceptive state after fertilization. With the knowledge that gamete membrane interactions occur in a stepwise fashion, sperm binding leading to sperm-egg fusion [57], experiments examined whether the sperm binding step of gamete membrane interactions was affected in membrane block establishment. Although the existence of a membrane block to polyspermy has been known for decades, and past work raised the possibility that the membrane block is due to reduced sperm binding to zygotes [44, 58], data here provide the clearest evidence to date that the membrane block is associated with the egg membrane having reduced capacity to support sperm binding. Moreover, we show that this postfertilization reduction of sperm binding does not occur to the same extent in fertilized prophase I oocytes. This study then sought to assess the mechanisms underlying this difference between metaphase II eggs and prophase I oocytes, examining the egg membrane protein CD9, which plays a role in gamete membrane interactions [59–62], and of the egg cortical cytoskeleton, which past work has implicated in the membrane block to polyspermy [52, 54].

MATERIALS AND METHODS

Collection of Oocytes and Eggs

All the work involving animals was conducted with approval from the Johns Hopkins University Animal Care and Use Committee. Throughout this work, the term oocyte is used to refer to the female gamete generically and to refer to germinal vesicle-intact, prophase I oocytes. The term egg connotes a female gamete arrested at metaphase II. Prophase I-arrested oocytes were collected from the ovaries of female CF-1 mice (Harlan) in Whitten medium (109.5 mM NaCl, 4.7 mM KCl, 1.2 mM KH_2PO_4, 1.2 mM $MgSO_4$, 5.5 mM glucose, 0.23 mM pyruvic acid, 4.8 mM lactic acid hemicalcium salt [63]) supplemented with 7 mM $NaHCO_3$ and 15 mM HEPES (hereafter referred to as Whitten-HEPES), and 0.05% polyvinyl alcohol (PVA; Sigma) and 0.25 mM dibutyryl cAMP (dbcAMP; Sigma). Cumulus cells were removed from oocytes by pipetting through a thin glass pipette, and then oocytes were transferred to culture drops of Whitten medium with 22 mM $NaHCO_3$ (hereafter referred to as Whitten-bicarbonate medium) with 0.05% PVA and 0.25 mM dbcAMP [64].

Metaphase II eggs were obtained by two methods. Prophase I oocytes were matured in vitro to metaphase II by washing the oocytes free of dbcAMP through six drops of Whitten-bicarbonate containing 0.05% PVA, then culturing the oocytes for ~14 h. In vivo matured (ovulated) metaphase II eggs were obtained from superovulated CF-1 female mice. Mice were injected with equine chorionic gonadotropin (eCG, 10 international units [IU]; Calbiochem/EMD Millipore, Billerica, MA), and then injected with human chorionic gonadotropin (hCG, 7.5 IU; Sigma) 48 h later to induce ovulation. Ovulated metaphase II eggs were collected from the oviducts of these mice at ~13 h post-hCG. Cumulus cells were removed by a brief (<5 min) incubation in Whitten-HEPES containing 3 mg/ml bovine serum albumin (BSA) (Albumax I; Gibco-BRL) and 0.25% type-IV S hyaluronidase (Sigma). The ZP were removed from oocytes and eggs by a brief incubation (<10 sec) in acidic culture medium compatible buffer (10 mM HEPES, 1 mM NaH_2PO_4, 0.8 mM $MgSO_4$, 5.4 mM KCl, 116.4 mM NaCl, pH 1.5). ZP-free oocytes and eggs were cultured for 60 min following ZP removal prior to IVF in Whitten-bicarbonate medium containing 0.05% PVA or 15 mg/ml BSA. Culture medium for prophase I oocytes also contained 0.25 mM dbcAMP to maintain prophase I arrest.

Conventional IVF of Prophase I Oocytes and Metaphase II Eggs

Sperm were collected from the caudae epididymides and vasa deferentia of male CD-1 retired breeders (Harlan) by a swim-up preparation in Whitten-bicarbonate medium with 15 mg/ml BSA as previously described [51]. The sperm concentration (in sperm/ml) was adjusted as necessary in Whitten-bicarbonate medium with 15 mg/ml BSA; medium also contained dbcAMP for insemination of prophase I oocytes (see methods below and/or figure legends for specific sperm concentrations for given experiments). Control experiments showed that IVF outcomes were comparable with metaphase II eggs in culture medium with and without dbcAMP (Fig. 1A).

ZP-free prophase I oocytes and in vitro matured metaphase II eggs were inseminated with capacitated sperm (sperm concentrations and inseminations times for various experiments noted in other sections and/or in figure legends).

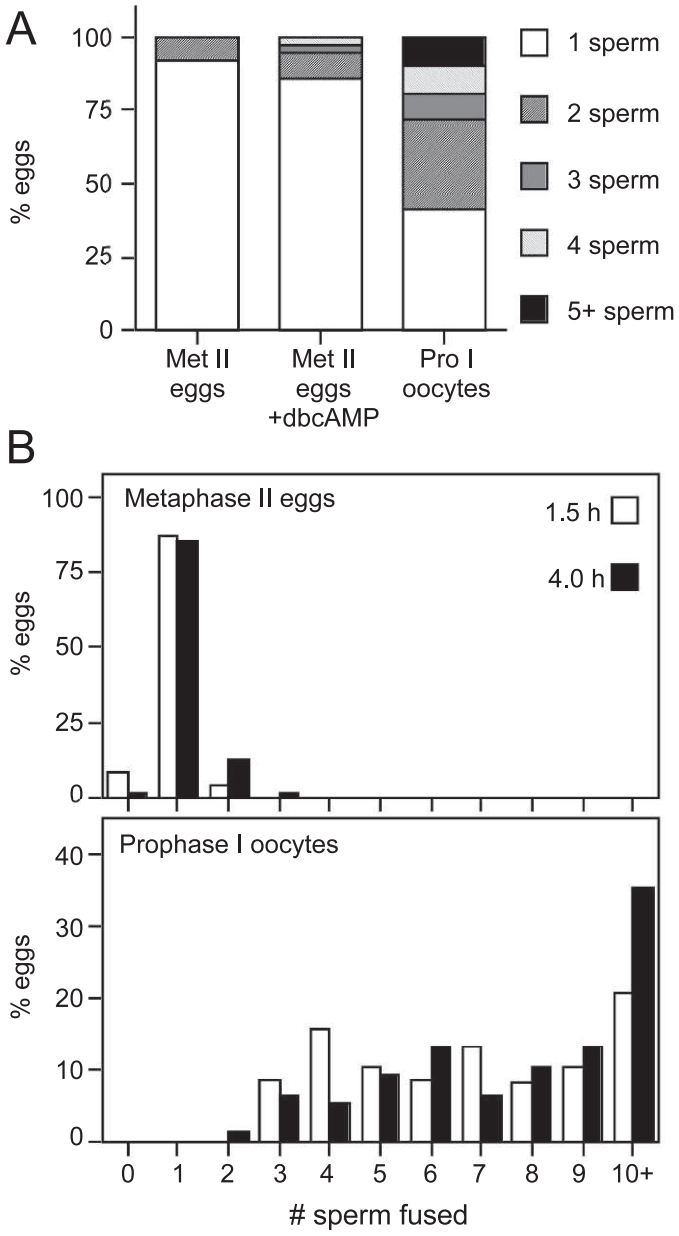

FIG. 1. ZP-free prophase I oocytes become highly polyspermic when inseminated. **A**) ZP-free in vitro matured metaphase II (Met II) eggs and prophase I (Pro I) oocytes were inseminated for 1.5 h with 50 000 sperm/ml, then assessed for the number of sperm fused per oocyte/egg (presented here as the percentages of oocytes/eggs that had one sperm fused, two sperm fused, etc., as indicated by the legend on the right). In all the studies here, prophase I oocytes were inseminated in the presence of dbcAMP to maintain prophase I arrest. As a control, experiments here included metaphase II eggs inseminated in the presence of dbcAMP to confirm that the increased extent of polyspermy in prophase I oocytes was not due to effects of dbcAMP. The average numbers of sperm fused per egg/oocyte (±SEM) were as follows: metaphase II eggs, 1.1 ± 0.045 (n = 38 eggs); metaphase II eggs + dbcAMP, 1.1 ± 0.071 (n = 36 eggs); prophase I oocytes, 2.3 ± 0.19 (n = 78 oocytes). **B**) ZP-free metaphase II eggs (upper panel) and prophase I oocytes (lower panel) were inseminated for 1.5 h (open bars) or 4.0 h (solid bars) with 100 000 sperm/ml, then assessed for the number of sperm fused per oocyte/egg. These graphs show frequency distributions, with the x axis indicating number of sperm fused and the y axis indicating the percentage of eggs with the indicated number of sperm fused. The average numbers of sperm per egg/oocyte (± SEM) were: metaphase II eggs at 1.5 h postinsemination, 0.96 ± 0.042 (n = 71 eggs); metaphase II eggs at 4 h postinsemination, 1.1 ± 0.045 (n = 81 eggs); prophase I oocytes at 1.5 h postinsemination, 7.3 ± 0.42 (n = 58 oocytes); prophase I oocytes at 4 h postinsemination, 8.5 ± 0.45 (n = 77 oocytes).

Experiments that assessed sperm binding to ZP-free prophase I oocytes and metaphase II eggs used 15 min inseminations with 500 000 sperm/ml, based on previous work [65–67]. After insemination, oocytes and eggs were washed free of loosely attached sperm. Assessments of sperm binding used carefully controlled washing conditions, washing oocytes/eggs through three drops of Whitten-bicarbonate containing 15 mg/ml BSA using a thin-bore pipette, with all the washes being performed by the same person using the same pipet and washing pressure [65–67]. Oocytes and eggs were then fixed in freshly prepared 3.7% paraformaldehyde in PBS and mounted in VectaShield (Vector Laboratories) containing 1 μg/ml 4′,6′-diamidino-2-phenylindole (DAPI; Sigma) to visualize the sperm DNA. In metaphase II eggs, the DNA of fused sperm in the egg cytoplasm undergoes decondensation and thus is easily distinguished from the condensed chromatin of sperm on the egg surface, whereas sperm DNA does not undergo decondensation in prophase I oocytes [16, 64, 68]. Therefore, in experiments here that examined fused sperm, inseminated prophase I oocytes were cultured for 3 h in medium lacking dbcAMP prior to fixation, allowing the sperm DNA in the oocyte cytoplasm to undergo decondensation as oocytes progressed from prophase I arrest. (In initial experiments to optimize conditions for this, inseminated prophase I oocytes were cultured in the absence of dbcAMP for 2.0–5.5 h; these experiments revealed 3 h was sufficient time for sperm decondensation.) We used this method preferentially over Hoechst- or DAPI-loading of oocytes/eggs to examine dye transfer to the fused sperm [69]; this dye-loading method is acceptable for use with live eggs and was used for certain experiments here (see below). However, this dye-loading method is difficult to use with fixed eggs because dye leakage can occur from fixed eggs, which can cause falsely positively stained sperm. In these experiments, we were examining large enough numbers of oocytes/eggs at one time such that fixation was essential to ensure that all the samples were precisely time-matched for postinsemination time.

Reinsemination Assay for Assessing Establishment of the Membrane Block to Polyspermy

Membrane block establishment was examined using a reinsemination assay essentially as previously described [51, 54, 70, 71]. Briefly, ZP-free eggs were inseminated to generate zygotes, and then these zygotes were challenged with a second batch of sperm to determine if sperm from this second batch were still able to penetrate the membrane. As a control, naive unfertilized eggs were inseminated with this second batch of sperm. In the studies here, metaphase II eggs and prophase I oocytes were inseminated with one batch of sperm (referred to as IVF1; 1 h insemination with 100 000 sperm/ml), washed to remove any loosely attached sperm, and then cultured for an additional 2, 4, or ~18–20 h (overnight), allowing time for establishment of a membrane block to polyspermy. After this culture period, the cells were challenged with a second batch of sperm, referred to as IVF2. For prophase I oocytes, the culture medium in all the steps was supplemented with 0.25 mM dbcAMP to maintain prophase I arrest.

Sperm used in these assays were labeled so that sperm from the first and second inseminations (IVF1 and IVF2, respectively) could be distinguished. Sperm were labeled with Alexa Fluor succinimidyl esters fluorescent dyes (Invitrogen); Alexa Fluor 546 (red) and Alexa Fluor 488 (green) were prepared as stocks in dimethyl sulfoxide at 10 mg/ml and stored in at −80°C in 3 μl aliquots. Sperm were collected by mincing one cauda epididymis and vas deferens of a CD-1 retired breeder male mouse (Harlan) in a 125 μl drop of Whitten-bicarbonate medium (without BSA or PVA) under mineral oil. The sperm were allowed to swim out of the tissue for 10 min, and the tissue was then removed. Alexa Fluor dye was then added to the sperm in the droplet to a final concentration of 0.2 mM; the sperm were then cultured in the dark for 60 min at 37°C in 5% CO_2 in air. After this incubation, the 125 μl of concentrated sperm were pipetted into the bottom of a 750 μl column of Whitten-bicarbonate medium containing 15 mg/ml BSA in a 12 × 75 mm polystyrene culture tube. This was incubated for 60 min, after which the top 220 μl of this column, containing the swim-up sperm, were placed in a fresh tube. The sperm were then cultured for an additional 1.5–2 h to allow sperm capacitation and acrosome exocytosis to occur.

For assessment of the extent of fertilization by IVF2 sperm, the oocytes or eggs were loaded with DAPI [69] by culturing in medium containing 20 μg/ml DAPI for the last 30 min of the culture period between IVF1 and IVF2. The oocytes and eggs were then inseminated for 60 min with Alexa Fluor 546-labeled sperm (150 000 sperm/ml in 10 μl drops with 10 oocytes per drop). After this second insemination (IVF2), the cells were pipetted into 100 μl drops of Whitten-bicarbonate containing 15 mg/ml BSA in 8 × 9 mm diameter Press-to-Seal silicone isolators (Grace Bio-Labs) on 55 × 24 mm microscope coverslips (5–6 cells per well). Oocytes and eggs were viewed on an inverted fluorescence microscope and scored for the number of red-labeled fused sperm.

Reinsemination Assay for Assessing Sperm Binding to the Plasma Membrane of Fertilized Metaphase II Eggs and Prophase I Oocytes

ZP-free prophase I oocytes and in vitro matured metaphase II eggs were inseminated to create zygotes as described above (referred to as IVF1; 60 min insemination with 100 000 sperm/ml), then cultured for an additional 1 h (for 2 h total since the start of IVF1) or an additional 4 h (for a total of 5 h since the start of IVF1). At this time, the zygotes were challenged with a second batch of sperm (IVF2), which were labeled with Alexa Fluor 546 (described above). Insemination conditions for these sperm binding assays were based on previous studies (15 min insemination, 500 000 sperm/ml [65–67]). After insemination, the cells were washed through three drops of Whitten-bicarbonate containing 15 mg/ml BSA using a thin-bore pipette to detach any loosely bound sperm; all the washes were performed by the same person using the same pipet and washing pressure. Cells were then fixed in 3.7% paraformaldehyde in PBS, then mounted in VectaShield-mounting medium containing 1.5 mg/ml DAPI to aid in the visualization of the sperm heads. The average numbers of red-labeled sperm bound per oocyte/egg were calculated for each group. For presentation of these data adjusted for the surface area of the microvillar surface, we calculated the microvillar surface to be ~13 000 μm^2 for a metaphase II egg and ~20 000 μm^2 for a prophase I oocyte, based on the diameter of the typical metaphase II egg being 75 μm and prophase I oocyte being 80 μm, and using a value of 75% of the total surface area of a metaphase II egg being covered in microvilli, based on published data [72–74].

In Vitro Fertilization of Oocytes and Eggs Treated with Anti-CD9 Antibody

ZP-free prophase I oocytes and in vitro matured metaphase II eggs were incubated for 60 min prior to insemination with 100 μg/ml of anti-CD9 monoclonal antibody KMC8.8 (diluted in Whitten-bicarbonate with 15 mg/ml BSA; 10 eggs per 10 μl drop) as we have done previously [67]. Control oocytes and eggs were incubated in parallel with 100 μg/ml nonimmune control rat immunoglobulin G (IgG) (Jackson Immunoresearch). Oocytes and eggs were then inseminated by adding sperm to a final concentration of 100 000 sperm/ml (by adding 10 μl of 200 000 sperm/ml to the 10 μl drop containing eggs and antibody). After a 60 min insemination, oocytes and eggs were washed free of loosely attached sperm, fixed, and mounted in DAPI-containing VectaShield as described above.

Oocyte/Egg-Conditioned Medium and Anti-CD9 Immunoblot Analysis

We examined if CD9-containing vesicles were released from prophase I oocytes and metaphase II eggs using the method of preparing oocyte/egg-conditioned medium described by Miyado et al. [75]. ZP-free prophase I oocytes, ovulated metaphase II eggs, and in vitro-matured metaphase II eggs were transferred immediately after ZP removal to 60 μl of Whitten-bicarbonate medium containing 0.05% PVA (40 cells/60 μl, as done by Miyado et al. [75]). Culture medium for prophase I oocytes contained 0.25 mM dbcAMP. The cells were cultured for 2 h, after which 60 μl of medium was pipetted into a microcentrifuge tube and deoxycholic acid (Sigma) was added for a final concentration of 0.1%. This mixture sat for 2–3 min and then was trichloroacetic acid (TCA) precipitated by adding one-tenth volume of 77% TCA, followed by a 30 min incubation on ice. Precipitated proteins were pelleted by centrifugation (4°C, 15 min, 10 000 × *g*), and washed with 300 μl of cold acetone, followed by a second centrifugation (4°C, 5 min, 10 000 × *g*). The pellet was then air-dried and resuspended in 10 μl of 2× SDS-PAGE sample buffer. As a positive control in these experiments, protein lysates of five metaphase II eggs were prepared for immunoblot analysis as was done previously [75]. These protein samples of eggs or oocyte/egg-conditioned medium were separated by SDS-PAGE and then immunoblotted with an anti-CD9 antibody (KMC 8.8 monoclonal antibody; 0.2 μg/ml) as previously described [67]. We also used another method of preparing oocyte/egg-conditioned medium, with a smaller volume of medium, 50% more eggs, and no precipitation step. ZP-free prophase I oocytes or metaphase II eggs were transferred immediately after ZP removal to 20 μl of Whitten-bicarbonate medium containing 0.05% PVA (40–60 cells/20 μl medium); the medium for prophase I oocytes contained 0.25 mM dbcAMP. The cells were cultured in the medium for 2 h, after which the 20 μl drop of oocyte/egg-conditioned medium was combined with 5 μl of 5× SDS-PAGE sample buffer. We did not detect significant CD9 in conditioned medium prepared in this way (data not shown).

Scanning Electron Microscopy and Micropipette Aspiration

Unfertilized and fertilized oocytes and eggs were prepared for scanning electron microscopy and viewed using an FEI Quanta 200 Environmental Scanning Electron Microscope with low-vacuum mode as previously described [76]. Micropipette aspiration to assess effective cortical tension was performed as previously described [77]. Micropipette aspiration is broadly applicable to many cell types [78] and is our preferred method because it is the most suitable cell mechanics measurement approach for cells the size of mouse oocytes. Studies comparing micropipette aspiration to microrheology (which measures very short time-scale mechanics) showed measurements made by these two methods to agree quantitatively [79–82]. Micropipette aspiration measures longer time-scale mechanics (>0.5 sec) and deforms the cortex over areas of a few tens of micrometers squared, thus averaging out shorter length-scale mechanics. In the experiments here, we compared cortical tension in unfertilized prophase I oocytes to fertilized prophase I oocytes (assessed at ~2 h postinsemination). In our previous work, we utilized various experimental treatments (e.g., cytochalasin D) to test hypotheses regarding functions of cytoskeletal proteins in regulating cortical tension [77]; we did not repeat the use of those experimental treatments found in our previous work in parallel with the studies of unfertilized and fertilized oocytes here.

Statistical Analyses

Statistical analyses using ANOVA with Fisher protected least significant difference post hoc testing, Mann-Whitney *U*-test, Kruskal-Wallis test complemented by Wilcoxon signed-rank test, or chi-squared (chi square) analyses were conducted using StatView 5.0 (SAS Institute). A P value less than 0.05 was considered significant.

RESULTS

ZP-Free Prophase I Oocytes Become Highly Polyspermic When Inseminated

Fertilization outcomes with ZP-free prophase I oocytes were investigated, comparing these to IVF outcomes with ZP-free metaphase II eggs. In 1.5 h inseminations with 50 000 sperm/ml, the extent of polyspermy was much higher with prophase I oocytes than it was with metaphase II eggs (Fig. 1A). These experiments included the control of inseminating metaphase II eggs in the presence of dbcAMP because prophase I oocytes needed to be cultured and inseminated in culture conditions that maintain high protein kinase A activity for prophase I arrest [64]. The IVF outcomes and extent of polyspermy were similar with metaphase II eggs with and without dbcAMP (Fig. 1A), demonstrating that that the increased extent of polyspermy in prophase I oocytes was not due to effects of dbcAMP.

Additional experiments examined sperm incorporation over time into prophase I oocytes and metaphase II eggs at two different postinsemination time points as we have used previously [51, 52]. In these assays of sperm incorporation over time, the postinsemination times were selected based on data that show that the membrane block to polyspermy in metaphase II eggs is established by 60–90 min postinsemination [42, 51]. This is also consistent with our previous studies showing that the number of sperm fused per metaphase II egg would plateau at ~1–2 sperm fused per egg between 1.5 and 4 h postinsemination (with variability associated with sperm concentration and sperm quality) [36, 51, 52]. In experiments here, metaphase II eggs had an average of 0.96 ± 0.042 sperm fused per egg at 1.5 h postinsemination and 1.1 ± 0.045 sperm fused per egg at 4 h postinsemination, consistent with previous observations [36, 51, 52]. Prophase I oocytes had significantly more sperm fused per oocyte, with 7.3 ± 0.42 sperm fused per oocyte at 1.5 h postinsemination and 8.5 ± 0.45 sperm used per oocyte at 4 h postinsemination. Figure 1B presents frequency distributions of the extent of polyspermy, showing that more than 90% of prophase I oocytes have four or more fused sperm at 1.5 and 4 h postinsemination, while only 12%

of metaphase II eggs were dispermic by 4 h postinsemination. These data suggest that prophase I oocytes maintained membrane receptivity after penetration by the first fertilizing sperm, and this contributed to a high extent of polyspermy.

ZP-Free Prophase I Oocytes Are Deficient in the Establishment of the Membrane Block to Polyspermy

The increased extent of sperm incorporation over time into ZP-free oocytes was suggestive of defects in membrane block establishment (Fig. 1B). To examine the membrane block more specifically, we utilized reinsemination assays, in which fertilized oocytes are tested to determine if they maintained the ability to be penetrated by sperm [51, 54, 70, 71]. In these experiments, prophase I oocytes and metaphase II eggs were inseminated (IVF1 in Fig. 2A), and then after a culture period, challenged with a fresh batch of sperm in a second insemination (IVF2). The key endpoint in these experiments was whether sperm from the second insemination could fertilize the zygotes, indicative of the zygote plasma membrane retaining receptivity to sperm. Sperm used in these assays were labeled with Alexa Fluor succinimidyl esters fluorescent dyes, using different colors for IVF1 and IVF2, so that sperm from the first and second inseminations could be distinguished (Fig. 2, A and B). Metaphase II eggs respond to a fertilizing sperm by down-regulating membrane receptivity to sperm; as noted above, this occurs by ~60–90 min after the first sperm penetrates [42, 51, 70, 71]. Thus, by the 3 and 5 h time points used here, very few IVF2 sperm from the second insemination were detected in zygotes derived from metaphase II eggs (Fig. 2C). The response of prophase I oocytes to fertilizing sperm was very different. Zygotes derived from prophase I oocytes contain significantly more IVF2 sperm than do zygotes derived from metaphase II eggs, most noticeably at the time point of 3 h after the start of IVF1 (Fig. 2C). These data are consistent with prophase I oocytes have a lesser ability as compared to metaphase II eggs to undergo a postfertilization down-regulation of membrane receptivity.

We next examined sperm binding specifically. The goals of these studies were to examine whether the difference in the extent of polyspermy in prophase I oocytes was due to an increased ability of the oocyte membrane to support sperm binding and to determine if prophase I oocytes differed in the extent of supporting sperm binding as compared to metaphase II eggs, either before or after fertilization. Additionally, these experiments were designed to address the fundamental question of whether reduced sperm binding to the zygote membrane accounts for the reduced membrane receptivity to sperm that develops after fertilization.

IVF experiments to assess sperm binding to ZP-free cells (15 min inseminations with 500 000 sperm/ml of unlabeled sperm) revealed that 22.0 ± 1.4 sperm bound per prophase I oocyte and 13.0 ± 1.0 sperm bound per metaphase II egg; a total of 61 metaphase II eggs and 47 prophase I oocytes were assessed in this series of experiments ($n = 3$). We evaluated whether the apparent increased extent of sperm binding to prophase I oocytes as compared to metaphase II eggs was linked to differences in membrane topography. The metaphase II egg is polarized; 70%–80% of the egg surface is the microvillar domain that supports sperm binding, and the remainder of the egg surface is the amicrovillar domain over the metaphase II spindle [72–74]. In contrast, the surface of a prophase I oocyte is uniformly covered with microvilli [83–85], and membrane proteins that participate in sperm-egg interaction are localized over the entire surface of prophase I oocytes, whereas they are enriched in the microvillar domain of metaphase II eggs [67, 86]. With the surface area of the microvillar surface estimated to be ~13 000 μm^2 for a metaphase II egg and ~20 000 μm^2 for a prophase I oocyte, we conclude that there are approximately similar extents of sperm binding per microvillar surface area between prophase I oocytes and metaphase II eggs (~1 sperm per 1000 μm^2).

Further experiments examined sperm binding to 2- and 5-h-old zygotes derived from metaphase II eggs and prophase I oocytes. The zygotes in these experiments were compared to control, culture time-matched unfertilized oocytes and eggs. Alexa Fluor-labeled sperm were used so that sperm from the first and second inseminations could be distinguished (as in Fig. 2). In these experiments, the binding of labeled sperm to unfertilized prophase I oocytes was ~3-fold higher as compared to unfertilized metaphase II eggs (11 ± 1.0 versus 3.9 ± 0.54 for the 2 h group; 5.1 ± 1.0 versus 1.6 ± 0.31 for the 5 h group; Fig. 3). The magnitude of this difference was greater with fertilized cells; sperm binding to zygotes derived from prophase I oocytes was 5–9-fold higher as compared to zygotes derived from metaphase II eggs (5.5 ± 0.78 versus 1.1 ± 0.24 for the 2-h-old zygotes; 1.1 ± 0.29 versus 0.13 ± 0.08 for the 5-h-old zygotes; Fig. 3). Most importantly, these studies also allowed us to compare sperm binding to unfertilized cells versus early zygotes, testing the hypotheses that sperm binding to zygotes would be reduced as compared to sperm binding to unfertilized eggs, and comparing this phenomenon in metaphase II eggs and prophase I oocytes. From the unfertilized to fertilized state, there was a decline in sperm binding, but this decline occurred more rapidly and to a greater extent in zygotes derived from metaphase II eggs as compared to zygotes derived from prophase I oocytes. For metaphase II eggs, sperm binding was reduced to 28% of control levels with 2-h-old zygotes and to 8% of control levels with 5-h-old zygotes, whereas for prophase I oocytes, sperm binding was reduced to 50% of control levels with 2-h-old zygotes and to 23% of control levels with 5-h-old zygotes (Fig. 3). These data are consistent with prophase I oocytes having a reduced ability to establish a membrane block to polyspermy, both in terms of timing and the extent of the reduction in sperm binding. Finally, these studies also show that there is a culture time-dependent decline in the ability of the membrane to support sperm binding. There is a ~50% decline in membrane receptivity to sperm between the 2 and 5 h time points with unfertilized metaphase II eggs and prophase I oocytes. It should be noted, however, that the extent of the time-dependent decline in sperm binding is greater with fertilized cells than with unfertilized cells (88% with fertilized metaphase II eggs; 79% with fertilized prophase I oocytes).

Involvement of CD9 in Fertilization of Prophase I Oocytes

We next sought to identify if differences in the functions of the membrane protein CD9 accounted for these differences between prophase I oocytes and metaphase II eggs. CD9 on the mouse egg membrane is near-essential for fertilization because *Cd9* deficiency is associated with severely impaired female fertility, with litter sizes reduced to 0%–60% of controls, and IVF studies showing drastic reductions in sperm-egg fusion with eggs from *Cd9*-deficieint females [59–62]. Pertinent to our work here comparing prophase I oocytes and metaphase II eggs, Miyado et al. [75] presented a difference between prophase I oocytes and metaphase II eggs related to CD9, specifically related to a recently speculated function of CD9 in fertilization through release of CD9 from the egg surface [87]; however, it is worth noting that this premise has been countered by other studies [88, 89]. Miyado et al. [75]

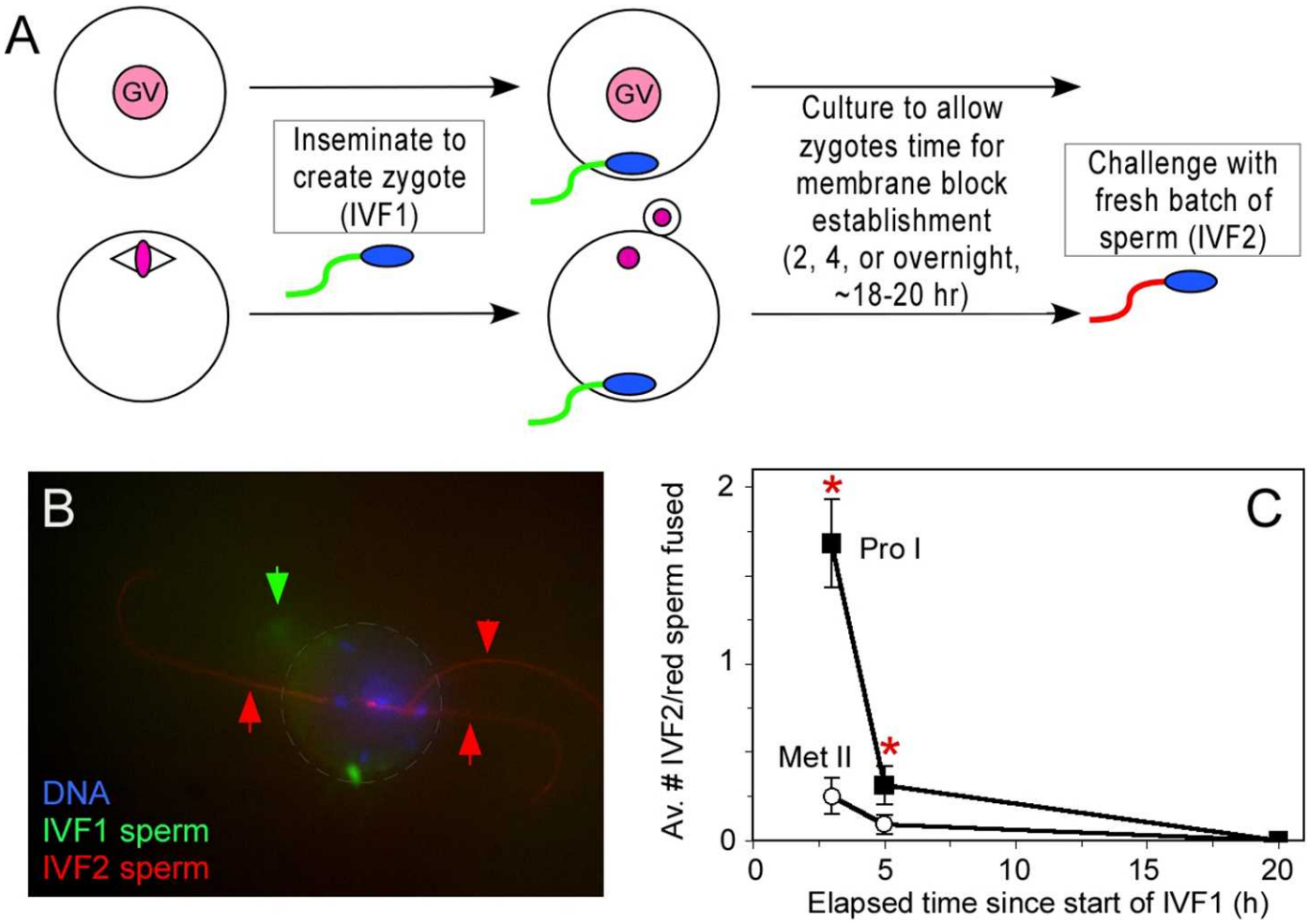

FIG. 2. Prophase I oocytes have an impaired ability to reduce membrane receptivity to sperm after fertilization, resulting in a membrane block to polyspermy. **A**) A schematic diagram of the experimental design. ZP-free metaphase II eggs and prophase I oocytes were inseminated (referred to as IVF1, which used a 60 min insemination with 100 000 sperm/ml that were labeled with Alexa Fluor 488). After this insemination, cells were washed to remove loosely attached sperm, and then cultured for an additional 2, 4, or 19 h (for a total of 3, 5, or 20 h after the start of IVF1). These fertilized eggs and oocytes were then challenged with Alexa Fluor 546 (red)-labeled sperm in a second insemination, or so-called reinsemination (shown in the figure as IVF2; 150 000 sperm/ml for 60 min). **B**) A representative prophase I oocyte from these reinsemination assays. DAPI-staining maternal DNA and multiple sperm heads are visible (blue), as are three Alexa Fluor 546-labeled sperm tails (red arrowheads); a green Alexa Fluor 488-labeled sperm is just out of the plane of focus (green arrow head). **C**) Average number of IVF2 sperm fused with respect to elapsed time since the start of IVF1 (in hours) for zygotes derived from metaphase II eggs (open circles) and from prophase I oocytes (solid squares), with red asterisks indicated a statistically significant difference between prophase I oocytes and metaphase II eggs ($P < 0.05$; ANOVA with Fisher protected least significant difference post hoc test). Data shown in **C** come from three to five experimental replicates, with 30–50 cells per experimental group). Control unfertilized metaphase II eggs that had been subjected to time-matched culture for 3 h had 2.1 ± 0.19 Alexa Fluor 546-labeled sperm fused per egg and for 5 h had 1.8 ± 0.24 Alexa Fluor 546-labeled sperm fused per egg. Control unfertilized prophase I oocytes that had been subjected to time-match culture for 3 h had 6.5 ± 0.59 Alexa Fluor 546-labeled sperm fused per egg and for 5 h had 3.8 ± 0.32 Alexa Fluor 546-labeled sperm fused per oocyte. The 20 h time point was not examined with unfertilized eggs because postovulatory aging affects the egg membrane's receptivity to sperm [70].

presented transmission electron microscopy data showing that release of exosome-like-containing vesicles was not detected from prophase I oocytes, whereas these vesicles were detected in metaphase II eggs. We wished to examine in CD9 function in prophase I oocytes more explicitly and therefore performed experiments to address two specific questions: (1) is fertilization of prophase I oocytes dependent on CD9, and (2) does CD9 release differ between prophase I oocytes and metaphase II eggs? The overall rationale behind these experiments was to determine if there were differences in the function of CD9 in fertilization between prophase I oocytes and metaphase II eggs, and in turn, if these could be associated with the difference in the oocyte's ability to establish a membrane block to polyspermy.

We tested the hypothesis that sperm fusion with prophase I oocytes might differ from metaphase II eggs in dependence on CD9. These experiments assessed the extent of fertilization of metaphase II eggs and prophase I oocytes treated with anti-CD9 antibodies; it has been well known that sperm interactions with metaphase II eggs were dramatically reduced in the presence of anti-CD9 antibodies [59, 67, 90]. The extent of fertilization of both prophase I oocytes and metaphase II eggs was decreased in the presence of anti-CD9 antibodies, as measured by the average number of sperm fused per oocyte, the percentage of oocytes that were fertilized, and the percentage of oocytes that were polyspermic (Fig. 4). These data indicate that fertilization of prophase I oocytes is mediated by CD9, as is the case for metaphase II eggs.

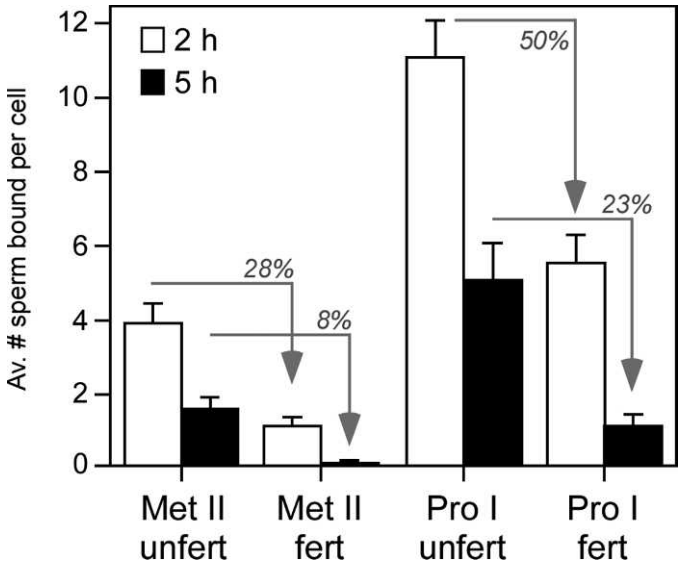

FIG. 3. Sperm binding to the plasma membrane of unfertilized and fertilized metaphase II eggs and prophase I oocytes. This graph shows the results of reinsemination assays (similar to that shown in Fig. 2) to assess sperm binding to the membranes of fertilized metaphase II eggs and prophase I oocytes. ZP-free metaphase II eggs (Met II) and prophase I oocytes (Pro I) were inseminated, then cultured for either a total of 2 h (open bars) or 5 h (solid bars); control unfertilized eggs and oocytes were cultured in parallel. Prophase I oocytes were cultured in medium containing dbcAMP to maintain prophase I arrest. These cells were then inseminated with a second batch of sperm (Alexa Fluor 546-labeled sperm, 500 000 sperm/ml, 15 min), washed, then fixed and assessed for the average number of sperm bound per egg/oocyte. Wilcoxon signed rank testing revealed statistically significant differences ($P < 0.05$) in the decrease in sperm binding observed with each pairwise set of unfertilized cells to early fertilized cells (pairwise comparisons indicated by gray arrows) and in the increase in sperm binding observed with each pairwise set of metaphase II eggs to compared to prophase I oocytes (not marked in figure). Sample sizes: unfertilized Met II eggs with 2 h culture, 39; unfertilized Met II eggs with 5 h culture, 19; fertilized Met II eggs with 2 h culture, 32; fertilized Met II eggs with 5 h culture, 30; unfertilized Pro I eggs with 2 h culture, 30; unfertilized Pro I eggs with 5 h culture, 15; fertilized Pro I eggs with 2 h culture, 33; fertilized Pro I eggs with 5 h culture, 28.

We next compared the release of CD9 from oocytes and eggs by assessing the amounts of CD9 in oocyte-conditioned medium from prophase I oocytes and metaphase II eggs, using the method previously described [75]. In these experiments, we examined two types of metaphase II eggs, those that were in vitro matured from prophase I oocytes and those collected following ovulation. Previous studies of these CD9 release phenomena had examined only ovulated eggs [75, 87], so we included ovulated eggs to be consistent with this past work. Surprisingly, we detected very little CD9 released from ovulated metaphase II eggs, in vitro matured metaphase II eggs or prophase I oocytes (Fig. 5). The previous report had shown that the amount of CD9 in egg-conditioned medium from 40 eggs was similar to or even higher than the amount of CD9 in five intact eggs [75]. In our studies, we detected substantially less CD9 release from 40 oocytes or eggs than what was detected in five intact eggs (Fig. 5). These results show that extent of CD9 release does not correlate with the extents of sperm-egg interaction and fertilization and are consistent with data from others suggesting that the release of CD9 from eggs does not play a critical role in fertilization [88, 89]. Moreover, our studies did not identify differences in the function of CD9 in fertilization between prophase I oocytes and metaphase II eggs.

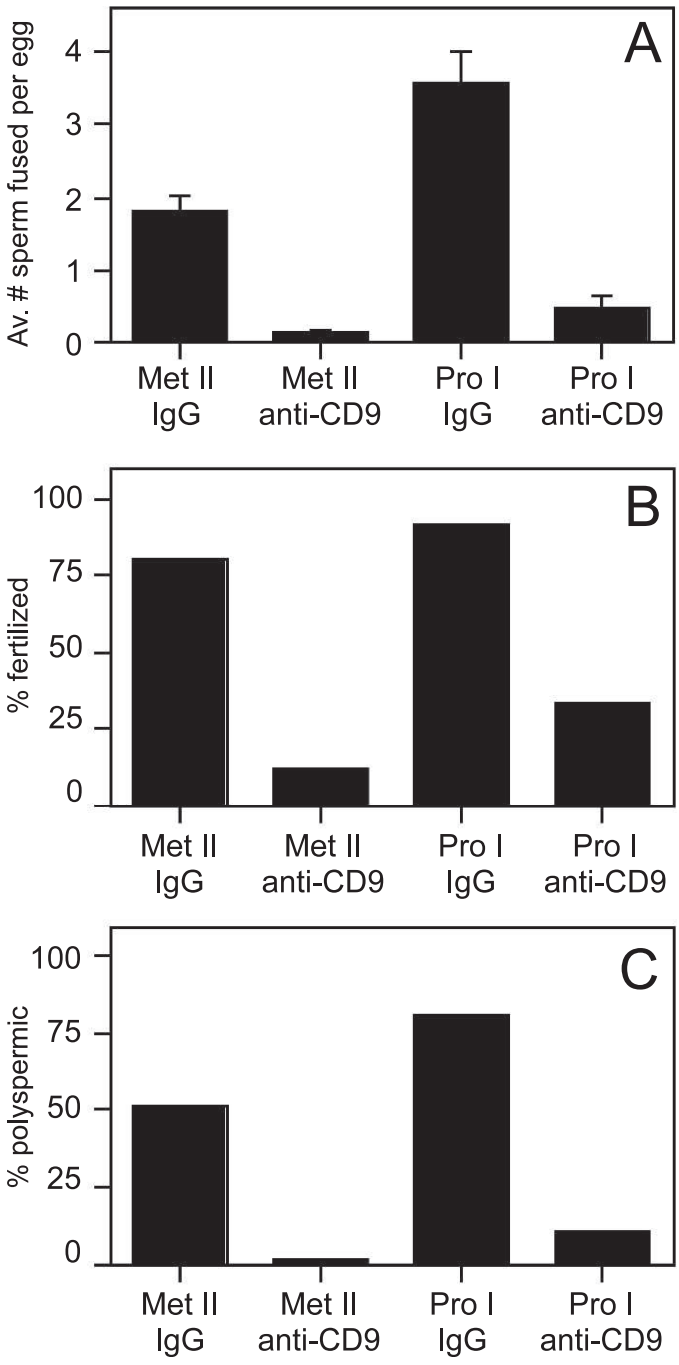

FIG. 4. Fertilization of prophase I oocytes is inhibited by anti-CD9 antibodies. ZP-free metaphase II eggs (Met II) and prophase I oocytes (Pro I) were incubated for 60 min with either 100 μg/ml anti-CD9 antibody or nonimmune control IgG (IgG), then inseminated (100 000 sperm/ml, 1.5 h). **A**) The average number of sperm fused per egg/oocyte. **B**) The percentage of fertilized eggs/oocytes (i.e., fertilized by least one sperm). **C**) The percentage of polyspermic eggs/oocytes (i.e., fertilized by two or more sperm). Sample sizes: metaphase II (Met II) eggs + nonimmune IgG, 47; metaphase II eggs + anti-CD9, 48; prophase I oocytes (Pro I) + nonimmune IgG, 36; prophase I oocytes + nonimmune IgG, 36; prophase I oocytes + anti-CD9, 36.

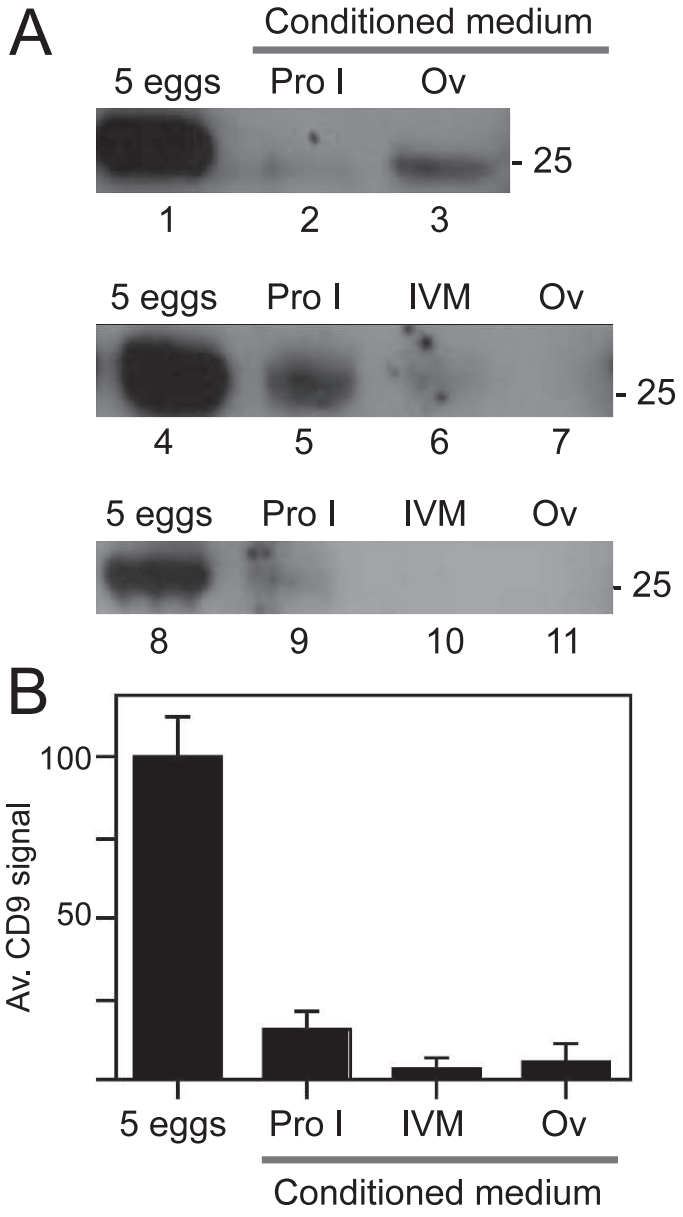

FIG. 5. Significant CD9 release is not detected from prophase I oocytes or metaphase II eggs. Conditioned medium from prophase I oocytes, in vitro matured metaphase II eggs (IVM), and ovulated MII eggs (Ov) was prepared as described (*Materials and Methods,* ref. [75]). **A**) Blots from three different experimental replicates. Lanes 1, 4, and 8 contain lysates from five ovulated MII eggs (labeled: 5 eggs); lanes 2, 5, and 9 contain prophase I oocyte-conditioned medium (labeled: Pro I); lanes 3, 7, and 11 contain ovulated MII egg-conditioned medium (labeled: Ov); lanes 6 and 10 contain in vitro matured MII egg-conditioned medium (labeled: IVM). **B**) The average signal intensities (±SEM) for each experimental group, expressed as a percentage of the 5 eggs control (defined as 100).

Membrane and Cortical Changes Associated with Fertilization Are Not Detected in Fertilized Prophase I Oocytes

Oocyte membrane topography changes dramatically with the progression through meiosis. Prophase I oocytes show a uniform distribution of microvilli over the oocyte surface; polarity develops following meiotic maturation to metaphase II, with the formation of an amicrovillar domain and an actin-rich cap over the metaphase II spindle [83–85]. In fertilized metaphase II eggs, additional remodeling of the egg membrane and underlying cortex occurs at the site of sperm incorporation, resulting in the formation of a fertilization cone over the sperm DNA; the fertilization cone is free of microvilli and enriched with actin in the cortex [91–94]. Our past work showed that fertilization cone formation was delayed in eggs fertilized by ICSI [54], of note because ICSI-fertilized eggs were deficient in the ability to establish a membrane block to polyspermy [54–56]. We therefore speculated that prophase I oocytes could have differences in sperm-induced membrane and cortical remodeling; we examined this by low-vacuum scanning electron microscopy [76]. Control fertilized metaphase II eggs showed clear signs of membrane remodeling, with the formation of an amicrovillar patch over the site of sperm incorporation (Fig. 6A), developing to a fertilization cone (Fig. 6, B and C), consistent with previously published work (e.g., [91–94]). In stark contrast, fertilized prophase I oocytes showed no signs of any sperm-induced membrane remodeling at postinsemination times at which metaphase II eggs had clear fertilization cones (2.5 h postinsemination, Fig. 6C–E; 1.5 h postinsemination also examined, data not shown). This failure of sperm-induced membrane remodeling was observed in 100% of fertilized prophase I oocytes examined ($n = 50$ oocytes).

An additional postfertilization change in metaphase II eggs is an increase in effective cortical tension, a metric that is a readout of biochemical, structural, and mechanical features of the cell cortex and specifically reflects both the tension and the stretch modulus of the cell [95, 96]. Our micropipette aspiration studies of mouse oocytes have detected a range of effects on cortical tension with experimental manipulations or differences in biological states. For example, we detected reductions of ~50% (with inhibition of myosin light chain kinase) to ~95% (with treatment with the actin-disrupting drug cytochalasin D) and increases of up to ~60% (with treatment with concanavalin A) [77]. Relevant to our interest in postfertilization membrane and cortical changes, we have detected a ~60% postfertilization increase in cortical tension in early embryos as compared to unfertilized metaphase II eggs [77]. However, we were not able to detect such a difference in cortical tension between unfertilized and fertilized prophase I oocytes. Unfertilized prophase I oocytes had an average effective cortical tension of 2.2 ± 0.18 nN/μm, and fertilized prophase I oocytes had an average effective cortical tension of 2.1 ± 0.16 nN/μm (not statistically significantly different, Mann-Whitney *U*-test; Fig. 7). The variability in these datasets (oocyte-to-oocyte, measurement-to-measurement) is similar to what we observed in our other analyses of cortical tension (e.g., see supplemental data published with reference [77]).

DISCUSSION

The data here indicate that the acquisition of activation competence, which occurs during meiotic maturation from prophase I to metaphase II, includes development of the ability to establish a membrane block to polyspermy. The data from the series of IVF experiments presented here show that the postfertilization reduction in membrane receptivity is both less robust and slower to develop in fertilized prophase I oocytes as compared to metaphase II eggs. An additional fundamental finding here is that the step of gamete membrane interactions that is altered postfertilization is the egg membrane's capacity to support sperm binding. This does not exclude the possibility that a decline in membrane fusibility also occurs, but the data here clearly provide an answer to the question of what step of gamete membrane interactions, binding or fusion, is altered on

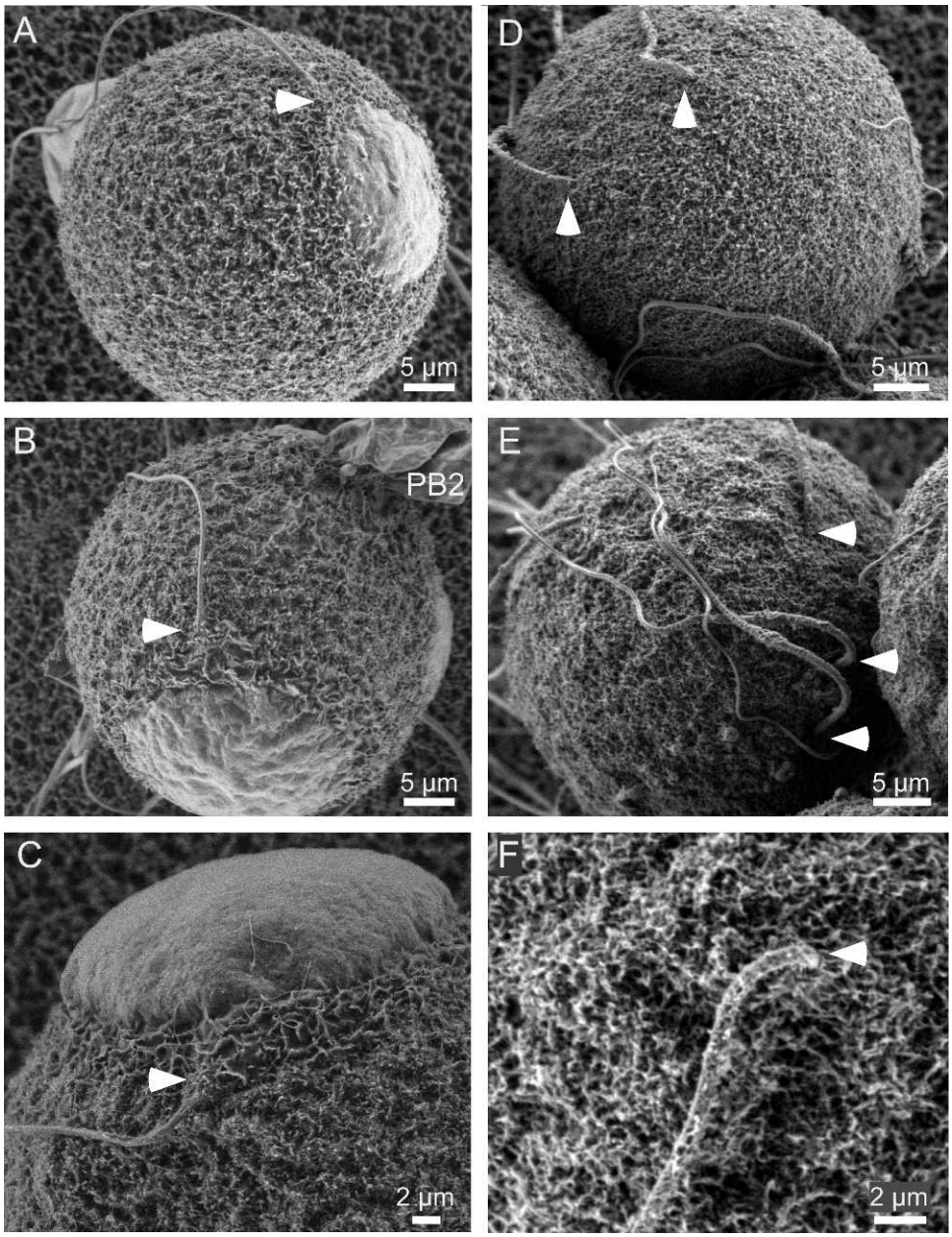

FIG. 6. Lack of postfertilization sperm-induced membrane remodeling in prophase I oocytes. Inseminated ZP-free metaphase II eggs (**A**, fixed at 1.25 h postinsemination [n = 38]; **B**, fixed at 1.5 h postinsemination [n = 18]; **C**, fixed at 2.5 h postinsemination [n = 23]) or prophase I oocytes (**D**–**F**, fixed at 2.5 h postinsemination [n = 50]) were viewed by low-vacuum scanning electron microscopy. Bars = 5 μm (**A**, **B**, **D**, and **E**) and 2 μm (**C** and **F**). Arrowheads mark the sites of sperm penetration into the oocyte/egg. Amicrovillar patches develop over the site of sperm incorporation in fertilized metaphase II eggs (**A**), which then develop into elevated fertilization cones (**B**, **C**), whereas amicrovillar patches are not observed at sperm incorporation sites in fertilized prophase I oocytes.

the zygote. While previous reports have suggested that the mammalian membrane block to polyspermy is due to reduced sperm binding [44, 58], the data here are the clearest to date that show that the membrane block is associated with the postfertilization egg membrane having reduced ability to support sperm binding. There also is a decline in membrane receptivity to sperm observed here with increased in vitro culture time with unfertilized eggs and oocytes, consistent with what has been observed with postovulatory aging in vivo [70]. However, this time-dependent decline is not as dramatic as fertilization-induced membrane changes. It is difficult to speculate about how a time-dependent decline in membrane receptivity to sperm compares to a fertilization-induced membrane block to polyspermy, but insights into the molecular characteristics associated with these functional changes will be important for shedding light on these phenomena.

The finding that the membrane block to polyspermy is associated with the zygote membrane being less supportive of sperm binding is consistent with data here showing that fertilization of prophase I oocytes is dependent on CD9. CD9 has been referred to as having a role in the overall process leading to sperm-egg fusion, but it is unclear if CD9 is specifically involved in membrane fusion or is a fusogen, and, on the other hand, there is evidence suggestive a role of CD9 in sperm-egg binding. *Cd9*-deficient eggs have a reduced ability to support the formation of strong adhesions with sperm [97],

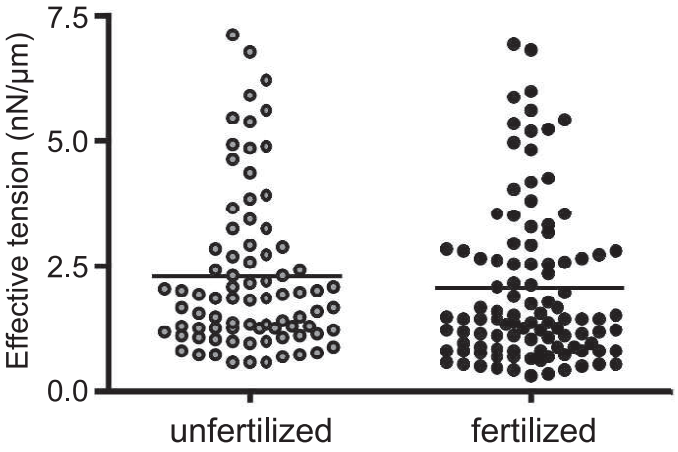

FIG. 7. Effective cortical tension in unfertilized and fertilization prophase I oocytes. Scatter plot of effective cortical tension, assessed by micropipette aspiration and measured in nN/μm [77], of unfertilized prophase I oocytes (n = 81; average effective tension = 2.2 ± 0.18 nN/μm) and fertilized prophase I oocytes (n = 104; average effective tension = 2.1 ± 0.16 nN/μm; $P > 0.05$, Mann-Whitney *U*-test).

in agreement with observations of sperm accumulating in the perivitelline space of *Cd9*-null eggs and only transiently attaching to the egg surface [62] and data from studies with function-blocking anti-CD9 antibodies indicative of a role of egg CD9 in adhesion strengthening [98]. It is also worth noting that the various proposed modes of CD9 action (exosomes, trogocytosis, adhesion strengthening, optimizing egg membrane order [57]) are not mutually exclusive. Data presented here differ from previously published data in support of the premise that CD9 functions in fertilization through release of CD9-containing exosome-like vesicles [75]. We are uncertain about why our results differ from those of Miyado et al. [75], although there are differences in mouse strains (CF-1 females were used in our work, and the studies of Miyado et al. that used wild-type eggs used C57BL/6 females). Our demonstration of little to no CD9 in oocyte- or egg-conditioned medium shows that significant CD9 release does not occur from all mouse oocytes and eggs, and despite this, these oocytes and eggs can still be fertilized.

A significant question about the membrane block to polyspermy is how does the fertilizing sperm trigger this change in the egg. As addressed in the *Introduction,* increased $[Ca^{2+}]_{cyt}$ facilitates membrane block establishment but is not sufficient [51, 54], making membrane block establishment different from most other egg activation events, nearly all of which are entirely Ca^{2+} dependent [99]. Although one model for membrane block establishment was that sperm-egg fusion and incorporation of the sperm membrane into the egg membrane is the trigger [55], the work here provides clear evidence that sperm-egg fusion is not sufficient to trigger normal membrane block establishment because sperm obviously fuse with prophase I oocytes and yet the membrane block response is significantly deficient. This indicates that the membrane block to polyspermy is a two-part process: the sperm provides the trigger, and the female gamete must be capable of responding to the fertilizing sperm. The data here on reduced responsiveness of prophase I oocytes complements other work documenting similar reduced responsiveness in postovulatory aged metaphase II eggs and in metaphase II eggs with suppressed Ca^{2+} signaling as a result of loading with the intracellular Ca^{2+} chelator BAPTA-AM (1,2-*Bis*(2-aminophenoxy)ethane-*N*,*N*,*N*′,*N*′-tetraacetic acid tetrakis-acetoxymethyl ester) [51, 70].

Adding to data suggesting a role of the egg actin cytoskeleton in the membrane block [52, 54], we show here that the deficiency in membrane block establishment correlates with two postfertilization membrane/cortical changes that are lacking in fertilized prophase I oocytes. One of these is a postfertilization change in effective cortical tension, which increases 1.6-fold from unfertilized metaphase II egg to 1.5-h-old zygote [77]. Such a change in effective cortical tension from unfertilized to fertilized prophase I oocyte is not detected here. Effective cortical tension is mediated by the organization of actin filaments, interfilament linkages, linkages between filaments and the plasma membrane, and force generation from actin assembly and the actin-associated motor myosin-II. These data on cortical tension in oocytes and eggs suggest that these cytoskeletal components in a metaphase II egg are in some way competent to undergo a fertilization-induced change and that this competence is lacking in a prophase I oocyte. The other postfertilization membrane/cortical change that is lacking in fertilized prophase I oocytes is sperm-induced cortical and membrane remodeling, namely the formation amicrovillar patches and then fertilization cones at the site of sperm incorporation. Considering that cell surface function, such as the ability to support sperm binding, is very likely affected by the cell cortex, these data provide rationale to consider postfertilization changes in the cortical cytoskeleton as part of membrane block establishment. Interestingly, this maturation of the oocyte cortex to an activation-competent form may be evolutionarily conserved. The postfertilization cortical contraction toward the egg animal pole that occurs in metaphase II anuran eggs does not occur in prophase I oocytes [100–103]. Taken together, these data indicate that cortical maturation is a component of cytoplasmic maturation during the oocyte-to-egg transition and that the egg cortex has to be appropriately primed and tuned to be responsive to a fertilizing sperm.

Understanding the causes of embryonic triploidy is highly relevant to improving reproductive health and success; this includes elucidating factors that contribute to prevention of polyspermic fertilization and conditions that could contribute to increased incidence of polyspermy. Polyspermy clearly occurs in vivo. Triploid embryos that are the result of polyspermic fertilization are recovered after natural matings [35, 38]. Triploidy occurs in ~1%–3% of all human conceptions [104–106], and diandric triploidy resulting from dispermic fertilization represents 60%–80% of triploids [104, 107–110]. Triploid conceptus material is detected in up to 30% of spontaneous abortions with embryonic aneuploidy [104, 107–109, 111–115]. Also of interest in the cell biology of fertilization, recent data provide foundations for an evolving model of the role(s) of primary sperm-ZP binding in fertilization [116–120], and thus raise the possibility that multiple mechanisms contribute to prevent polyspermy, complementing the well-known actions of cortical granule release on the ZP [24, 25]. The prevention of polyspermic fertilization is a multifaceted process, involving the contribution of the female tract managing sperm numbers at the site of fertilization, as well as the egg's own preventive mechanisms of converting the ZP and the plasma membrane to unreceptive states. The cellular and molecular mechanisms underlying the postfertilization decline in egg membrane receptivity to sperm are still poorly understood, but the differences identified here between postfertilization responses in metaphase II eggs and prophase I oocytes can provide clues to guide future studies

into the mechanistic basis of the membrane block to polyspermy.

ACKNOWLEDGMENT

We gratefully acknowledge the assistance of the Johns Hopkins Biostatistics Center and the Johns Hopkins Integrated Imaging Center.

REFERENCES

1. Conti M, Hsieh M, Zamah AM, Oh JS. Novel signaling mechanisms in the ovary during oocyte maturation and ovulation. Mol Cell Endocrinol 2012; 356:65–73.
2. Kubiak JZ. Mouse oocytes gradually develop the capacity for activation during the metaphase II arrest. Dev Biol 1989; 136:537–545.
3. Berrios M, Bedford JM. Oocyte maturation: aberrant post-fusion responses of the rabbit primary oocyte to penetrating spermatozoa. J Cell Sci 1979; 39:1–12.
4. Ajduk A, Malagocki A, Maleszewski M. Cytoplasmic maturation of mammalian oocytes: development of a mechanism responsible for sperm-induced Ca2+ oscillations. Reprod Biol 2008; 8:3–22.
5. Chiba K. Evolution of the acquisition of fertilization competence and polyspermy blocks during meiotic maturation. Mol Reprod Dev 2011; 78:808–813.
6. Mehlmann LM, Kline D. Regulation of intracellular calcium in the mouse egg: calcium release in response to sperm or inositol trisphosphate in enhanced after meiotic maturation. Biol Reprod 1994; 51:1088–1098.
7. Shiraishi K, Okada A, Shirakawa H, Nakanishi S, Mikoshiba K, Miyazaki S. Developmental changes in the distribution of the endoplasmic reticulum and inositol 1,4,5-triphosphate receptors and the spatial pattern of Ca2+ release during maturation of hamster oocytes. Dev Biol 1995; 170:594–606.
8. Jones KT, Carroll J, Whittingham DG. Ionomycin, thapsigargin, ryanodine, and sperm induced Ca2+ release increase during meiotic maturation of mouse oocytes. J Biol Chem 1995; 270:6671–6677.
9. Tombes RM, Simerly C, Borisy GG, Schatten G. Meiosis, egg activation, and nuclear envelope breakdown are differentially reliant on Ca2+, whereas germinal vesicle breakdown is Ca2+ independent in the mouse oocyte. J Cell Biol 1992; 117:799–811.
10. Mehlmann LM, Terasaki M, Jaffe LA, Kline D. Reorganization of the endoplasmic reticulum during meiotic maturation of the mouse oocyte. Dev Biol 1995; 170:607–615.
11. Mehlmann LM, Mikoshiba K, Kline D. Redistribution and increase in cortical inositol 1,4,5-trisphosphate receptors after meiotic maturation of the mouse oocyte. Dev Biol 1996; 180:489–498.
12. Fissore RA, Longo FJ, Anderson E, Parys JB, Ducibella T. Differential distribution of inositol trisphosphate receptor isoforms in mouse oocytes. Biol Reprod 1999; 60:49–57.
13. Xu Z, Williams CJ, Kopf GS, Schultz RM. Maturation-associated increase in IP3 receptor type 1: role in conferring increased IP3 sensitivity and Ca^{2+} oscillatory behavior in mouse eggs. Dev Biol 2003; 254:163–171.
14. Abbott AL, Fissore RA, Ducibella T. Identification of a translocation deficiency in cortical granule secretion in preovulatory oocytes. Biol Reprod 2001; 65:1640–1647.
15. FitzHarris G, Marangos P, Carroll J. Changes in endoplasmic reticulum structure during mouse oocyte maturation are controlled by the cytoskeleton and cytoplasmic dynein. Dev Biol 2007; 305:133–144.
16. Szollosi D, Szollosi MS, Czoloska R, Tarkowski AK. Sperm penetration into immature mouse oocytes and nuclear changes during maturation: an EM study. Biol Cell 1990; 69:53–64.
17. McLay DW, Clarke HJ. The ability to organize sperm DNA into functional chromatin is acquired during meiotic maturation in murine oocytes. Dev Biol 1997; 186:73–84.
18. Steeves CL, Hammer M-A, Walker GB, Rae D, Stewart NA, Baltz JM. The glycine neurotransmitter transporter GLYT1 is an organic osmolyte transporter regulating cell volume in cleavage-stage embryos. Proc Natl Acad Sci U S A 2003; 100:13982–13987.
19. Tartia AP, Rudraraju N, Richards T, Hammer M-A, Talbot P, Baltz JM. Cell volume regulation is initiated in mouse oocytes after ovulation. Development 2009; 136:2247–2254.
20. Baltz JM, Zhou C. Cell volume regulation in mammalian oocytes and preimplantation embryos. Mol Reprod Dev 2012; 79:821–831.
21. Iwamatsu T, Chang MC. Factors involved in the fertilization of mouse eggs in vitro. J Reprod Fert 1971; 26:197–208.
22. van der Ven HH, Al-Hasani S, Diedrich K, Hamerich U, Lehmann F, Krebs D. Polyspermy in in vitro fertilization of human oocytes: frequency and possible causes. Ann N Y Acad Sci 1985; 442:88–95.
23. Bleil JD, Wassarman PM. Mammalian sperm-egg interaction: fertilization of mouse eggs triggers modification of the major zona pellucida glycoprotein, ZP2. Dev Biol 1981; 86:189–197.
24. Abbott AL, Ducibella T. Calcium and the control of mammalian cortical granule exocytosis. Front Biosci 2001; 6:D792–D806.
25. Florman HM, Ducibella T. Fertilization in mammals. In: Neill JD (ed.), Knobil and Neill's Physiology of Reproduction, 3rd ed. San Diego: Elsevier; 2006:55–112.
26. Moore HD, Bedford JM. Ultrastructure of the equatorial segment of hamster spermatozoa during penetration of oocytes. J Ultrastruct Res 1978; 62:110–117.
27. Ducibella T, Duffy P, Reindollar R, Su B. Changes in the distribution of mouse oocyte cortical granules and ability to undergo the cortical reaction during gonadotropin-stimulated meiotic maturation and aging in vivo. Biol Reprod 1990; 43:870–876.
28. Wang W, Hosoe M, Li R, Shioya Y. Development of the competence of bovine oocytes to release cortical granules and block polyspermy after meiotic maturation. Dev Growth Differ 1997; 39:607–615.
29. Wang WH, Hosoe M, Shioya Y. Induction of cortical granule exocytosis of pig oocytes by spermatozoa during meiotic maturation. J Reprod Fertil 1997; 109:247–255.
30. Wu H, He CL, Fissore RA. Injection of a porcine sperm factor triggers calcium oscillations in mouse oocytes and bovine eggs. Mol Reprod Dev 1997; 46:176–189.
31. Abbott AL, Fissore RA, Ducibella T. Incompetence of preovulatory mouse oocytes to undergo cortical granule exocytosis following induced calcium transients. Dev Biol 1999; 207:38–48.
32. Tsai PS, van Haeften T, Gadella BM. Preparation of the cortical reaction: maturation-dependent migration of SNARE proteins, clathrin, and complexin to the porcine oocyte's surface blocks membrane traffic until fertilization. Biol Reprod 2011; 84:327–335.
33. Lewis WH, Wright ES. On the early development of the mouse egg. Carnegie Inst Contrib Embryol 1935; 25:113–143.
34. Odor DL, Blandau RJ. The frequency of supernumerary sperm in rat ova. Anat Rec 1949; 104:1–11.
35. Austin CR. The Mammalian Egg. Springfield, IL: Charles C. Thomas; 1961.
36. Gardner AJ, Evans JP. Mammalian membrane block to polyspermy: new insights into how mammalian eggs prevent fertilisation by multiple sperm. Reprod Fertil Dev 2006; 18:53–61.
37. Pincus G, Enzmann EV. Fertilisation in the rabbit. J Exp Biol 1932; 9: 403–408.
38. Austin CR, Braden AWH. An investigation of polyspermy in the rat and rabbit. Aust J Biol Sci 1953; 6:674–693.
39. Hunter RH. Fertilization of pig eggs in vivo and in vitro. J Reprod Fertil Suppl 1990; 40:211–226.
40. Sengoku K, Tamate K, Horikawa M, Takaoka Y, Ishikawa M, Dukelow WR. Plasma membrane block to polyspermy in human oocytes and preimplantation embryos. J Reprod Fertil 1995; 105:85–90.
41. Hunter RH, Vajta G, Hyttel P. Long-term stability of the bovine block to polyspermy. J Exp Zool 1998; 280:182–188.
42. Wolf DP. The block to sperm penetration in zona-free mouse eggs. Dev Biol 1978; 64:1–10.
43. Zuccotti M, Yanagimachi R, Yanagimachi H. The ability of hamster oolemma to fuse with spermatozoa: its acquisition during oogenesis and loss after fertilization. Development 1991; 112:143–152.
44. Horvath PM, Kellom T, Caulfield J, Boldt J. Mechanistic studies of the plasma membrane block to polyspermy in mouse eggs. Mol Reprod Dev 1993; 34:65–72.
45. Maluchnik D, Borsuk E. Sperm entry into fertilised mouse eggs. Zygote 1994; 2:129–131.
46. Jaffe LA, Gould M. Polyspermy-preventing mechanisms. In: Metz CB, Monroy A (eds.), Biology of Fertilization: the Fertilization Response of the Egg, vol. 3. Orlando, FL: Academic Press; 1985:223–250.
47. Miyazaki S, Igusa Y. Fertilization potential in golden hamster eggs consists of recurring hyperpolarizations. Nature 1981; 290:702–704.
48. Igusa Y, Miyazaki S, Yamashita N. Periodic hyperpolarizing responses in hamster and mouse eggs fertilized with mouse sperm. J Physiol 1983; 340:633–647.
49. Jaffe LA, Sharp AP, Wolf DP. Absence of an electrical polyspermy block in the mouse. Dev Biol 1983; 96:317–323.
50. McCulloh DH, Rexroad CE Jr, Levitan H. Insemination of rabbit eggs is associated with slow depolarization and repetitive diphasic membrane potentials. Dev Biol 1983; 95:372–377.
51. Gardner AJ, Williams CJ, Evans JP. Establishment of the mammalian

membrane block to polyspermy: evidence for calcium-dependent and -independent regulation. Reproduction 2007; 133:383–393.
52. McAvey BA, Wortzman GB, Williams CJ, Evans JP. Involvement of calcium signaling and the actin cytoskeleton in the membrane block to polyspermy in mouse eggs. Biol Reprod 2002; 67:1342–1352.
53. Wolf DP, Nicosia SV, Hamada M. Premature cortical granule loss does not prevent sperm penetration of mouse eggs. Dev Biol 1979; 71:22–32.
54. Wortzman-Show GB, Kurokawa M, Fissore RA, Evans JP. Calcium and sperm components in the establishment of the membrane block to polyspermy: studies of ICSI and activation with sperm factor. Mol Human Reprod 2007; 13:557–565.
55. Maleszewski M, Kimura Y, Yanagimachi R. Sperm membrane incorporation into oolemma contributes to the oolemma block to sperm penetration: evidence based on intracytoplasmic sperm injection experiments in the mouse. Mol Reprod Dev 1996; 44:256–259.
56. Sengoku K, Tamate K, Takaoka Y, Horikawa M, Goishi K, Okada R, Tsuchiya K, Ishikawa M. Requirement of sperm-oocyte plasma membrane fusion for establishment of the plasma membrane block to polyspermy in human pronuclear oocytes. Mol Reprod Dev 1999; 52: 183–188.
57. Evans JP. Sperm-egg interaction. Annu Rev Physiol 2012; 74:477–502.
58. Wolf DP, Hamada M. Sperm binding to the mouse egg plasmalemma. Biol Reprod 1979; 21:205–211.
59. Miyado K, Yamada G, Yamada S, Hasuwa H, Nakamura Y, Ryu F, Suzuki K, Kosai K, Inoue K, Ogura A, Okabe M, Mekada E. Requirement of CD9 on the egg plasma membrane for fertilization. Science 2000; 287:321–324.
60. Le Naour F, Rubinstein E, Jasmin C, Prenant M, Boucheix C. Severely reduced female fertility in CD9-deficient mice. Science 2000; 287: 319–321.
61. Kaji K, Oda S, Shikano T, Ohnuki T, Uematsu Y, Sakagami J, Tada N, Miyazaki S, Kudo A. The gamete fusion process is defective in eggs of CD9-deficient mice. Nat Genet 2000; 24:279–282.
62. Rubinstein E, Ziyyat A, Prenant M, Wrobel E, Wolf JP, Levy S, Le Naour F, Boucheix C. Reduced fertility of female mice lacking CD81. Dev Biol 2006; 290:351–358.
63. Whitten WK. Nutrient requirements for the culture of preimplantation embryos in vitro. Adv Biosci 1971; 6:129–139.
64. Cho WK, Stern S, Biggers JD. Inhibitory effect of dibutyryl cAMP on mouse oocyte maturation in vitro. J Exp Zool 1974; 187:383–386.
65. Redkar AA, Olds-Clarke PJ. An improved mouse sperm-oocyte plasmalemma binding assay: studies on characteristics of sperm binding in medium with or without glucose. J Androl 1999; 20:500–508.
66. Zhu X, Bansal NP, Evans JP. Identification of key functional amino acids of the mouse fertilin β (ADAM2) disintegrin loop for cell-cell adhesion during fertilization. J Biol Chem 2000; 275:7677–7683.
67. Glazar AI, Evans JP. IgSF8 (EWI-2) and CD9 in fertilization: evidence of distinct functions for CD9 and a CD9-associated protein in mammalian sperm-egg interaction. Reprod Fertil Dev 2009; 21:293–303.
68. Usui N, Yanagimachi R. Behavior of hamster sperm nuclei incorporated into eggs at various stages of maturation, fertilization, and early development. The appearance and disappearance of factors involved in sperm chromatin decondensation in egg cytoplasm. J Ultrastr Res 1976; 57:276–288.
69. Conover JC, Gwatkin RBL. Pre-loading of mouse oocytes with DNA-specific fluorochrome (Hoechst 33342) permits rapid detection of sperm oocyte-fusion. J Reprod Fert 1988; 82:681–690.
70. Wortzman GB, Evans JP. Membrane and cortical abnormalities in post-ovulatory aged eggs: analysis of fertilizability and establishment of the membrane block to polyspermy. Mol Hum Reprod 2005; 11:1–9.
71. Gardner AJ, Knott JG, Jones KT, Evans JP. CaMKII can participate in but is not sufficient for the establishment of the membrane block to polyspermy in mouse eggs. J Cell Physiol 2007; 212:275–280.
72. Eager DD, Johnson MH, Thurley KW. Ultrastructural studies on the surface membrane of the mouse egg. J Cell Sci 1976; 22:345–353.
73. Nicosia SV, Wolf DP, Inoue M. Cortical granule distribution and cell surface characteristics in mouse eggs. Dev Biol 1977; 57:56–74.
74. Longo FJ. Fine structure of the mammalian egg cortex. Am J Anat 1985; 174:303–315.
75. Miyado K, Yoshida K, Yamagata K, Sakakibara K, Okabe M, Wang X, Miyamoto K, Akutsu H, Kondo T, Takahashi Y, Ban T, Ito C, et al. The fusing ability of sperm is bestowed by CD9-containing vesicles released from eggs in mice. Proc Natl Acad Sci U S A 2008; 105:12921–12926.
76. Dalo DT, McCaffery JM, Evans JP. Ultrastructural analysis of egg membrane abnormalities in post-ovulatory aged eggs. Int J Dev Biol 2008; 52:535–544.
77. Larson SM, Lee HJ, Hung PH, Matthews LM, Robinson DN, Evans JP. Cortical mechanics and meiosis II completion in mammalian oocytes are mediated by myosin-II and Ezrin-Radixin-Moesin (ERM) proteins. Mol Biol Cell 2010; 21:3182–3192.
78. Hochmuth RM. Micropipet aspiration of living cells. J Biomech 2000; 33:15–22.
79. Girard KD, Chaney C, Delannoy M, Kuo SC, Robinson DN. Dynacortin contributes to cortical viscoelasticity and helps define the shape changes of cytokinesis. EMBO J 2004; 23:1536–1546.
80. Girard KD, Kuo SC, Robinson DN. Dictyostelium myosin II mechanochemistry promotes active behavior of the cortex on long time scales. Proc Natl Acad Sci U S A 2006; 103:2103–2108.
81. Yang L, Effler JC, Kutscher BL, Sullivan SE, Robinson DN, Iglesias PA. Modeling cellular deformations using the level set formalism. BMC Syst Biol 2008; 2:68.
82. Reichl EM, Robinson DN. Putting the brakes on cytokinesis with alpha-actinin. Dev Cell 2007; 13:460–462.
83. Nicosia SV, Wolf DP, Mastrioanni L Jr. Surface topography of mouse eggs before and after insemination. Gamete Res 1978; 1:145–155.
84. Wassarman PM, Ukena TE, Josefowicz WJ, Karnovsky MJ. Asymmetrical distribution of microvilli in cytochalasin B-induced pseudocleavage of mouse oocytes. Nature 1977; 265:742–744.
85. Longo FJ, Chen DY. Development of surface polarity in mouse eggs. Scan Electron Microsc 1984; Pt 2:703–716.
86. Evans JP, Foster JA, McAvey BA, Gerton GL, Kopf GS, Schultz RM. The effects of perturbation of cell polarity on molecular markers of sperm-egg binding sites on mouse eggs. Biol Reprod 2000; 62:76–84.
87. Barraud-Lange V, Naud-Barriant N, Bomsel M, Wolf JP, Ziyyat A. Transfer of oocyte membrane fragments to fertilizing spermatozoa. FASEB J 2007; 21:3446–3449.
88. Gupta S, Primakoff P, Myles DG. Can the presence of wild-type oocytes during insemination rescue the fusion defect of CD9 null oocytes? Mol Reprod Dev 2009; 76:602.
89. Barraud-Lange V, Boissonnas CC, Serres C, Auer J, Schmitt A, Lefevre B, Wolf JP, Ziyyat A. Membrane transfer from oocyte to sperm occurs in two CD9-independent ways that do not supply the fertilising ability of Cd9-deleted oocytes. Reproduction 2012; 144:53–66.
90. Chen MS, Tung KSK, Coonrod SA, Takahashi Y, Bigler D, Chang A, Yamashita Y, Kincade PW, Herr JC, White JM. Role of the integrin associated protein CD9 in binding between sperm ADAM 2 and the egg integrin $\alpha_6\beta_1$: implications for murine fertilization. Proc Natl Acad Sci U S A 1999; 96:11830–11835.
91. Lopata A, Sathananthan AH, McBain JC, Johnston WI, Speirs AL. The ultrastructure of the preovulatory human egg fertilized in vitro. Fertil Steril 1980; 33:12–20.
92. Brunet S, Maro B. Cytoskeleton and cell cycle control during meiotic maturation of the mouse oocyte: integrating time and space. Reproduction 2005; 130:801–811.
93. Maro BB, Johnson MH, Pickering SJ, Flach G. Changes in actin distribution during fertilization of the mouse egg. J Embryol Exp Morph 1984; 81:211–237.
94. Phillips DM, Shalgi R. Sperm penetration into rat ova fertilized in vivo. J Exp Zool 1982; 221:373–378.
95. Derganc J, Božic B, Sventina S, Žekš B. Stability analysis of micropipette aspriation of neutrophils. Biophys J 2000; 79:153–162.
96. Reichl EM, Ren Y, Morphew MK, Delannoy M, Effler JC, Girard KD, Divi S, Iglesias PA, Kuo SC, Robinson DN. Interactions between myosin and actin crosslinkers control cytokinesis contractility dynamics and mechanics. Curr Biol 2008; 18:471–480.
97. Jégou A, Ziyyat A, Barraud-Lange V, Perez E, Wolf JP, Pincet F, Gourier C. CD9 tetraspanin generates fusion competent sites on the egg membrane for mammalian fertilization. Proc Natl Acad Sci U S A 2011; 108:10946–10951.
98. Zhu X, Evans JP. Analysis of the roles of RGD-binding integrins, α_4/α_9 integrins, α_6 integrins, and CD9 in the interaction of the fertilin β (ADAM2) disintegrin domain with the mouse egg membrane. Biol Reprod 2002; 66:1193–1202.
99. Miao Y-L, Williams CJ. Calcium signaling in mammalian egg activation and embryo development: the influence of subcellular localization. Mol Reprod Dev 2012; 79:742–756.
100. Elinson RP. Site of sperm entry and a cortical contraction associated with egg activation in the frog *Rana pipiens*. Dev Biol 1975; 47:257–268.
101. Elinson RP. Fertilization of immature frog eggs: cleavage and development following subsequent activation. J Embryol Exp Morph 1977; 37:187–201.
102. Stewart-Savage J, Grey RD. The temporal and spatial relationships between cortical contraction, sperm trail formation, and pronuclear

migration in fertilized Xenopus eggs. Wilhelm Roux's Arch 1982; 191: 241–245.
103. Wolf DP. The cortical response in Xenopus laevis ova. Dev Biol 1974; 40:102–115.
104. Jacobs PA, Angell RR, Buchanan IM, Hassold TJ, Matsuyama AM, Manuel B. The origin of human triploids. Ann Human Genet 1978; 42: 49–57.
105. Jacobs PA, Szulman AE, Funkhouser J, Matsuura JS, Wilson CC. Human triploidy: relationship between parental origin of the additional haploid complement and development of partial hydatidiform mole. Ann Hum Genet 1982; 46:223–231.
106. Zaragoza MV, Surti U, Redline RW, Millie E, Chakravarti A, Hassold TJ. Parental origin and phenotype of triploidy in spontaneous abortions: predominance of diandry and association with the partial hydatidiform mole. Am J Hum Genet 2000; 66:1807–1820.
107. Meulenbroek GH, Geraedts JP. Parental origin of chromosome abnormalities in spontaneous abortions. Hum Genet 1982; 62:129–133.
108. Uchida IA, Freeman VC. Triploidy and chromosomes. Am J Obstet Gynecol 1985; 151:65–69.
109. Redline RW, Hassold T, Zaragoza MV. Prevalance of the partial molar phenotype in triploidy of maternal and paternal origin. Hum Pathol 1998; 29:505–511.
110. McFadden DE, Robinson WP. Phenotype of triploid embryos. J Med Genet 2006; 43:609–612.
111. Hassold T, Chen N, Funkhouser J, Jooss T, Manuel B, Matsuura J, Matsuyama A, Wilson C, Yamane JA, Jacobs PA. A cytogenetic study of 1000 spontaneous abortions. Ann Human Genet 1980; 44:151–178.
112. Boué J, Phillippe E, Giroud A, Boué A. Phenotypic expression of lethal anomalies in human abortuses. Teratology 1976; 14:3–20.
113. Creasy MR, Crolla JA, Alberman ED. A cytogenetic study of human spontaneous abortions using banding techniques. Hum Genet 1976; 31: 177–196.
114. Rehder H, Coerdt W, Eggers R. Klink F, Schwinger E. Is there a correlation between morphological and cytogenetic findings in placental tissue from early missed abortions? Hum Genet 1989; 82:377–385.
115. Brajenovic-Milic B, Petrovic O, Kraševic M, Ristic S, Kapovic M. Chromosomal anomalies in abnormal human pregnancies. Fetal Dian Ther 1998; 13:187–191.
116. Jin M, Fujiwara E, Kakiuchi Y, Okabe M, Satouh Y, Baba SA, Chiba K, Hirohashi N. Most fertilizing mouse spermatozoa begin their acrosome reaction before contact with the zona pellucida during in vitro fertilization. Proc Natl Acad Sci U S A 2011; 108:4892–4896.
117. Nishimura H, Kim E, Nakanishi T, Baba T. Possible function of the ADAM1a/ADAM2 fertilin complex in the appearance of ADAM3 on the sperm surface. J Biol Chem 2004; 279:34957–34962.
118. Tokuhiro K, Ikawa M, Benham AM, Okabe M. Protein disulfide isomerase homolog PDILT is required for quality control of sperm membrane protein ADAM3 and male fertility. Proc Natl Acad Sci U S A 2012; 109:3850–3855.
119. Kuzan FB, Fleming AD, Seidel GE Jr. Successful fertilization in vitro of fresh intact oocytes by perivitelline (acrosome-reacted) spermatozoa of the rabbit. Fertil Steril 1984; 41:766–770.
120. Inoue N, Satouh Y, Ikawa M, Okabe M, Yanagimachi R. Acrosome-reacted mouse sperm recovered from the perivitelline space can fertilize other eggs. Proc Natl Acad Sci U S A 2011; 108:20008–20011.